Characterization of pitting corrosion of stainless steel using artificial neural networks

M. J. Jiménez-Come*, I. J. Turias, J. J. Ruiz-Aguilar and F. J. Trujillo

In this work, different classification models were proposed to predict the pitting corrosion status of AISI 316 L stainless steel according to the environmental conditions and the breakdown potential values. In order to study the pitting corrosion status of this material, polarization tests were undertaken in different environmental conditions: varying chloride ion concentration, pH and temperature. Two different techniques were presented: *k* nearest neighbor (KNN) and artificial neural networks (ANNs). The parameters for the classifiers were set based on a compromise between recall and precision using bootstrap as validation technique. The ROC space was presented to compare the classification performance of the different models. In this frame, Bayesian regularized neural network model proved to be the most promising technique to determine the pitting corrosion status of 316 L stainless steel without resorting to optical metallographic studies.

1 Introduction

Stainless steels are iron-based alloys containing at least 11% of chromium. The existence of different grades of this alloy makes stainless steel one of the most diverse materials in terms of composition, mechanical properties and microstructure. For this reason, a wide range of applications are found for stainless steels, ranging from transportation and chemical industries to construction [1,2].

Austenitic stainless steel is one of the most popular grades of stainless steel due to its excellent corrosion resistance, its fire resistance, its high retention of strength, its low maintenance cost and its ability to be recycled [3]. However, this material may suffer corrosion under aggressive conditions, most notably, in those environments with chlorides and high temperature [4]. Corrosion can be defined as the degradation of a material through its contact with the environment. This has become an important economic problem in engineering applications [5,6]. Among the different types of corrosion, pitting corrosion is one of the most dangerous corrosion types for metallic alloys. This type of localized corrosion occurs at a microscopic level leading to irreversible failures in the properties of the material. Pitting corrosion can be difficult to detect, predict, and design against, as the complexity of the corrosive environment increases.

M. J. Jiménez-Come, I. J. Turias, J. J. Ruiz-Aguilar, F. J. Trujillo
University of Cadiz. Polytechnic School of Engineering (Algeciras), Avda. Ramón Puyol s/n. 11202 Algeciras/Cádiz, Spain
E-mail: mariajesus.come@uca.es

Based on ASTM-G150, the potentiostatic technique is an efficient tool to evaluate the pitting corrosion resistance of stainless steels. According to this norm, the susceptibility of the material to suffer pitting corrosion may be determined by evaluating the conditions when the current density reaches $100\,\mu A/cm^2$. The potential at this point is defined as the breakdown potential [7]. The breakdown potential is used as a general term to indicate the breakdown of the passive layer. It is used regardless the reaction that causes the breakdown of the passive layer: pitting or transpassive corrosion [8]. On one hand, when the breakdown is caused by pitting, the potential at $100\,\mu A/cm^2$ is called pitting potential [9,10]. On the other hand, when the transpassive area is reached without pits, authors assume that the material is not susceptible to pitting. Thus, in order to confirm the pitting attack after the polarization tests, authors analyze the material surface microscopically. However, the visual interpretation of the surface may lead to subjectivity in the results [11]. This work aims to solve this drawback and it presents an automatic way based on artificial intelligent techniques to detect pitting attack without requiring metallographic analysis of the material surface.

Different works about corrosion modelling can be found in the literature [12–14]. Among all the modelling techniques, artificial neural networks (ANNs) have been applied as an efficient tool in material science, characterization and testing. *Mirzadeh* et al. [15] used ANNs to model the effect of cold working temperature, the deformation, the strain rate and the initial austenitic grain size on the volume fraction of strain-induced martensite in stainless steel. In the study developed by *Cottis* et al. [16], a neural network model was presented to analyze

 © 2015 WILEY-VCH Verlag GmbH & Co. KGaA, Weinheim

atmospheric corrosion. In this work, the corrosion depth was estimated as a function of temperature, time of wetness, sulphur dioxide concentration, chloride concentration and exposure time. *Diaz* and *Lopez* [17] provided a function based on artificial neural networks to study corrosion penetration in carbon steel. *Ok* et al. [18] developed a model based on artificial neural networks to investigate the effects of pitting corrosion on the strength reduction of plates. *Cavanaugh* et al. [19] developed models based on neural networks to model pit growth of metallic alloys as a function of temperature, pH, chloride concentration and exposure time. *Parthiban* et al. [20] presented a back-propagation neural network to predict pitting potential values for different conditions of the steel in concrete in order to recognize the behavior of the material. *Lajevardi* et al. [21] presented a system to predict failure time as a consequence of stress corrosion cracking of 304 austenitic stainless steel in aqueous chloride solutions using ANNs.

Based on our previous studies about modelling behavior of stainless steels [22–24], and referring to the works presented in the literature review, the models based on artificial intelligence techniques have become a useful tool to be applied in the corrosion studies. In this sense, this work presents different models based on artificial neural networks, including the analysis about the influence of the Bayesian regularization in order to predict pitting status of 316 L stainless steel (1 when the material suffers pitting attack and 0 for no pitting attack). The models were used to predict the pitting status of this material based on the most critical environmental variables involved in pitting corrosion and the breakdown potential values, not requiring microscopic analysis after polarization test.. This study was based on the experimental data from an European project called "Avoiding catastrophic corrosion failure of stainless steel" – CORINOX -(RFSR-CT-2006–00022), partly developed in ACERINOX.

Firstly, this paper provides a description of the proposed classification models. The Methodology section exposes how the database for modelling was obtained, including a description of the validation technique used as well as a brief description of the statistical metrics selected to evaluate the classification performance and gives the experimental procedure. Results and Discussion section presents the results of the best classification models analyzing the optimal ANN topology. To conclude, principal remarks are exposed in the Conclusion section.

2 Methodology

2.1 The database

Several methods have been developed to study pitting corrosion such as potentiostatic, potentiokinetic or galvanostatic methods [25–27]. In this work, the breakdown potential values were determined by the potentiodynamic polarization curves. A specific electrochemical cell based on the Avesta design was used to evaluate pitting corrosion susceptibility. The principle of this cell is the use of a constant flow of distilled water (approximately 5–6 ml/h) in the crevice between the sample and the cell elements to avoid crevice corrosion that permits the determination of the breakdown potential accurately [9]. Additionally, a water flow from a thermostat bath circulates through the jacket of the cell, allowing the tests to be performed at different temperatures for each sample tested. A saturated calomel electrode (SCE) was used as a reference electrode whereas two graphite bars were used as the counter electrodes. All the specimens were cut into 40 mm x 40 mm and for all of them (the working electrode), the test surface was limited to be 1 cm^2, according to the cell design. All the samples were wet ground with 600 grit abrasive paper before immersion. During

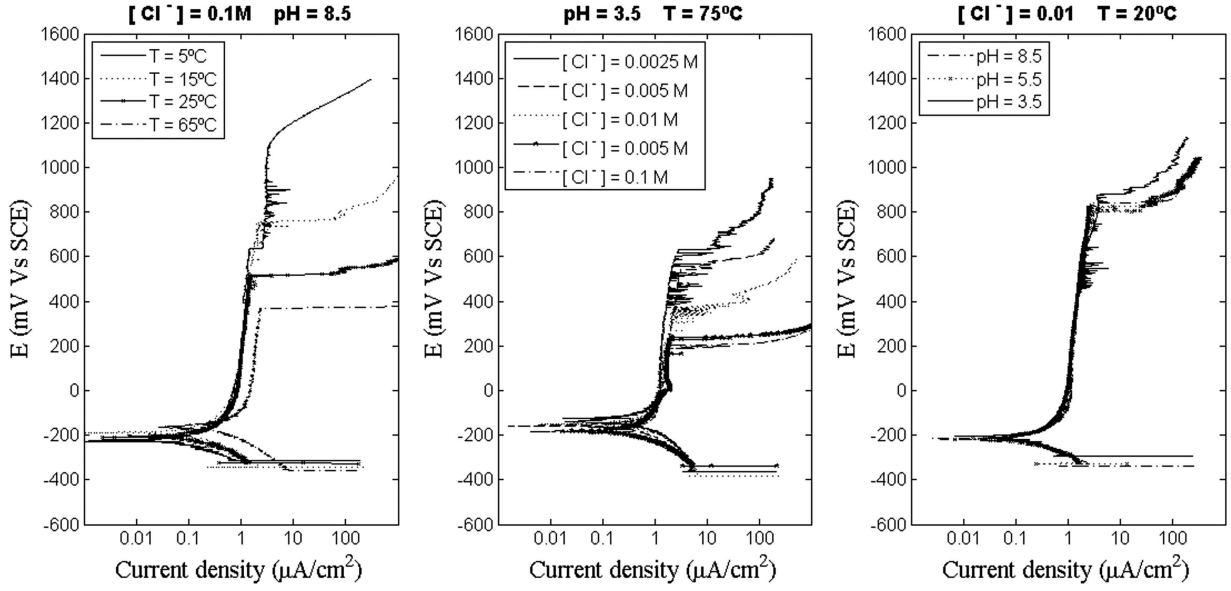

Figure 1. Polarization curves measured for AISI 316 L stainless steel using NaCl as precursor salt. a) [Cl^-]: 0.1 M, pH = 8.5; b) pH = 3.5, T = 75 °C; c) [Cl^-]: 0.1 M, T = 15 °C

© 2015 WILEY-VCH Verlag GmbH & Co. KGaA, Weinheim

Table 1. Environmental conditions for polarization tests of grade 316 L austenitic stainless steel

Total number of samples tested: 73		
pH	Chloride ion concentration [M]	Temperature (°C)
3.5	0.1 – 0.05 – 0.01 – 0.005 – 0.0025	2–75
5.5	0.1 – 0.05 – 0.01 – 0.005 – 0.0025	2–75
8.5	0.1 – 0.05 – 0.01 – 0.005 – 0.0025	2–75

the test, the electrolyte solution was mechanically stirred and deaerated with pure nitrogen flow (0.8 l/min). Before starting the test, all the specimens were cathodically polarized at a conditioning potential of −1300 mV for 180 seconds in an initial stage. Then, the potential scan was initiated at −1100 mV. The scan rate is an important parameter to consider in these experiments since high scan rates lead to high breakdown potentials, whereas lower values lead to more reliable results. Therefore, the scan rate was set to be 0.17 mVs^{-1} [28]. Figure 1 depicts different polarization curves obtained in NaCl aqueous solutions, where the breakdown potential can be defined in terms of potential at which the current density shows an increase, typically at 100 $\mu A/cm^2$.

In order to study the influence of the most relevant environmental factors on pitting corrosion resistance of grade 316 L stainless steel [19,29] different conditions were tested varying chloride ion concentration, pH and temperature. A total of 73 samples were collected. All the tested conditions are collected in Table 1.

After the polarization test, each specimen was examined in an optical microscope to check pitting attack in order to analyze the corrosion properties of the material (see Fig. 2). In this way, each pattern was characterized by the environmental conditions, its breakdown potential and labelled according to the corrosion status: 1 when pits were observed on the surface and 0, otherwise. In order to ensure reproducibility, each condition was tested three times. All the data were collected based on the experimental work of the European project called "Avoiding catastrophic corrosion failure of stainless steel" (RFSR-CT-2006–00022), a database for modelling pitting corrosion status was created. This database was used to develop a qualitative prediction model of pitting corrosion, taking into account the relationships between the environmental variables and the breakdown potential values obtained from the polarization tests.

2.2 Classification models

Different classification models were proposed to predict the pitting corrosion status of AISI 316 L stainless steel by an automatic way, without requiring metallographic studies: *k* nearest neighbor (as benchmark model) and artificial neural networks (ANNs).

2.2.1 Artificial neural networks

Artificial neural networks are powerful information processing tools with the ability to study complex nonlinear processes [30]. Multilayer neural networks are based on the combination of processing units, commonly referred to as neurons. These units are logically arranged into two or more layers. The layers between input and output are called hidden layers. The data are presented to the input layer whereas the output layer gives the modelled response. Each neuron in the network is connected to all neurons located in the following layer. These connections are associated to different weight factor determining the strength of the influence between the interconnected neurons [31].

During the learning process, the networks study the relationship between input-output pairs by adapting their connections, reducing the total error obtained between the target value and the predicted one (Equation (1)). The total error may be minimized in the learning stage using an adequate algorithm [32]. *Levenberg-Marquardt* [33] is the most widely used optimization algorithm.

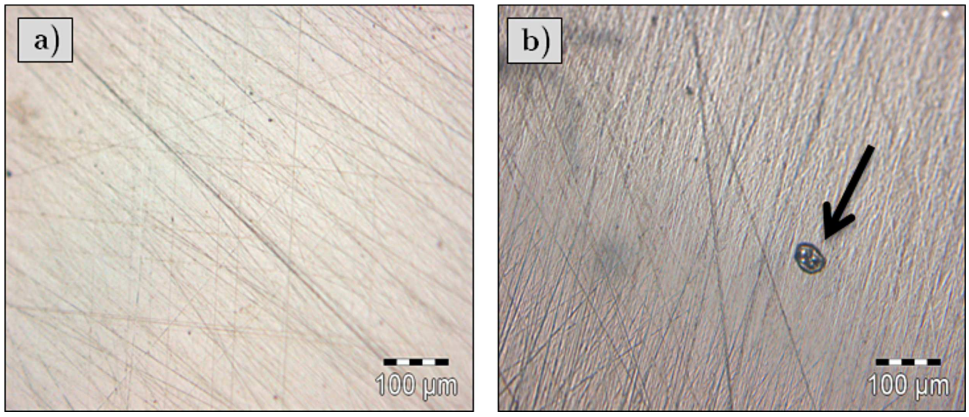

Figure 2. Images from optical microscopy analysis of austenitic stainless steel AISI 316 L after polarization test: a) No pitting attack, b) Pitting attack

© 2015 WILEY-VCH Verlag GmbH & Co. KGaA, Weinheim

$$E_D = \sum_{i=1}^{n}(y_i - t_i)^2 = \sum_{i=1}^{n} e_i^2 \quad (1)$$

Where n is the number of neurons while y and t are the predicted and target values, respectively.

The ANN presented in this paper is a backpropagation neural network (BPNN). This type of neural network learns from heuristic results by modifying the weights of the neurons based on the errors between the modelled output and the target value [34]. However, this technique may present some problems such as the selection of the optimal number of hidden neurons or the influence of initial choice of weight values on the classification performance. In this context, Bayesian learning was suggested as an effective option to deal with these drawbacks. In this study, the framework developed by *Mackay* was applied for the implementation of the Bayesian learning [35]. This method adapts the prior probability distribution into posterior probability distribution based on the patterns taking part into the training set.

Basically, a Bayesian neural network is a back propagation network with an additional term in the error function called the regularization parameters. These terms, introduced by *Tikhonov* [36], penalize the network complexity.

$$S(w) = \beta E_D + \alpha E_W \quad (2)$$

with,

$$E_W = \sum_{i=1}^{m} w_i^2 \quad (3)$$

The terms α and β are called the regularization parameters, whereas E_w is the penalty term. This parameter is included in order to penalize large values of the m weights. The ratio α/β controls the effective complexity of the network. Therefore, the correct selection of this regularization ratio is crucial within the regularization method. In the Bayesian framework, the weights are chosen based on the maximization of the conditional probability. Assuming a Gaussian form for the probabilities, the terms α and β can be defined as:

$$\alpha^{MP} = \frac{\gamma}{2E_w(x^{MP})} \quad (4)$$

$$\beta^{MP} = \frac{N - \gamma}{2E_D(x^{MP})} \quad (5)$$

where x^{MP} are the weights that maximize the posterior density and γ, the effective number of parameters, is given by:

$$\gamma = n - 2\alpha^{MP} tr(H^{MP})^{-1} \quad (6)$$

where n is the total number of parameters and H^{MP} is the Hessian matrix evaluated at $x^{MP.}$

2.3 Validation techniques

The use of artificial intelligence techniques in engineering applications has increased over the last years. In this context, the choice of the evaluation technique is crucial. Classification models assign automatically a pattern to one of the existing classes based on its different attributes. When the class of the pattern to be classified is known before the analysis of the data, the process is called supervised learning. In this way, it is possible to estimate the performance of the classifier by comparing the modelled response to the target value [37].

Smets and *Bogaerts* [38] recognized that data collection and the training step are the two principal steps to be considered in the prediction of the corrosion characterization behavior of materials. In their work, they focused their attention on the critical role of the learning and evaluation techniques. They tried to identify the most adequate method for the problem under study. In the presented work, bootstrap was presented as a validation technique to train the model. In this case, the training set is created by resampling with replacement. This step is repeated several times and different models are built from each bootstrap sample. The classifier is evaluated using a test sample with the patterns that have not been included in the training step. In this case, the error is calculated as an averaged error:

$$err^{Bt} = \frac{1}{M}\sum_{j=1}^{M} err_j^{Bt} \quad (7)$$

where M is the number of samples. *Efron* and *Tibshirani* [39] have compared the properties of this estimator with cross-validation estimators in theoretical and empirical ways. They affirm that the bootstrap estimator is biased upwards although it presents lower variability compared to cross-validation. To solve this drawback, *Efron* proposed the 0.632bootstrap estimator, given by the Equation (8):

$$err^{B632} = 0.632 \cdot err^{Bt} + 0.368 \cdot err \quad (8)$$

2.4 Performance evaluation

The statistical metrics used to evaluate the classification performance in this study were precision and recall:

- Precision, in the classification models, can be defined as the relation of the number of true positive (TP: number of the original corrosion samples classified correctly) divided by the total number of positive patterns classified by the model, including those which have been wrongly classified as positive (TP + FP), where FP is the number of the original corrosion samples that have not been classified correctly:

$$\text{Precision} = \frac{TP}{TP + FP} \quad (9)$$

- Recall is related to the sensitivity of the classifier. This term is defined by the number of true positive divided by the total

© 2015 WILEY-VCH Verlag GmbH & Co. KGaA, Weinheim

number of patterns belonging to the positive class (P: number of the original corrosion samples).

$$\text{Recall} = \frac{TP}{P} \tag{10}$$

3 Experimental procedure

A reliable prediction of pitting corrosion status is fundamental to identify pitting corrosion properties of austenitic stainless steel. In order to study the effect of different environmental conditions such as chloride ion concentration, pH and temperature, different samples of AISI 316 L stainless steel were subjected to polarization tests. A total of 77 observations composed the database using NaCl as precursor salt to create a model for determining pitting attack on the material surface by an automatic way.

The tested conditions are collected in Table 1. The environmental conditions and the breakdown potential values obtained for each sample were used as inputs to model pitting corrosion status of the material. The pitting corrosion status defined after each experiment by using an optical microscope was used to define the output of the models (1 when pits are observed on the material surface and 0, otherwise). Hence, each pattern was described by chloride ion concentration, pH, temperature, breakdown potential and a boolean value discerning the cases where pitting occurred. Additionally, in order to improve the accuracy of the models, all the original variables were linearly scaled to fit within the interval [−1 1].

The difficulty for the visual interpretation of the material surface after polarization tests that may lead to subjectivity in the results justifies the application of the classification models based on artificial intelligence techniques. Two different methods were studied in this paper: KNN using different values of *k* parameter (k = 1,3,5) and ANN models with different number of hidden neurons (1,2,5,10,20) and two activation functions for the hidden and output layers: tan-sigmoid and purelin transfer functions, respectively. In order to get the optimal structure, three-layer BPNNs with different numbers of hidden units were studied, analyzing the influence of the Bayesian regularization. The number of input neurons was given by the number of parameters studied for each pattern (chloride ion concentration, pH, temperature and the breakdown potential value) while the number of output neurons was given by the corrosion status defined by optical microcopic analysis (1-pitting corrosion) / (0-no pitting corrosion).

In order to analyze the classification performance of the different proposed models, bootstrap was applied as a validation technique. This iterative process was repeated 40 times in order to ensure the generalization capability of the model. The statistical indices were measured for each iteration and then averaged. In addition, the values of precision and recall obtained for each model were subjected to Friedman test, in order to calculate the statistically significant effects of the parameters involved in the model at $p < 0.05$.

4 Results and discussion

In order to analyze pitting corrosion status of austenitic stainless steel in different environmental conditions, different classification models were presented: KNN and ANNs trained with *Levenberg-Marquardt* and considering the Bayesian regularization. All the models were trained using bootstrap as validation technique.

Figure 3 shows box plots for the recall values of the classifiers presented in this paper to predict pitting corrosion status of 316 L austenitic stainless steel. This figure shows six statistic samples for each model: the average (black star), the median, the minimum and maximum recall values indicated by the ends of the vertical lines and the upper and lower quartiles. The upper boundary of the box locates the 75th percentile while the lower boundary indicates the 25th percentile. In some cases, outliers were represented as well. These points (represented by crosses) are extreme values that deviate from the rest of the sample.

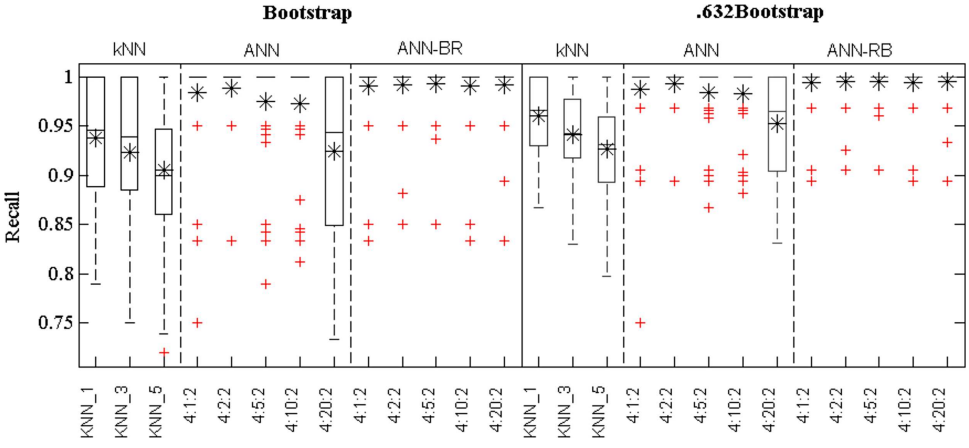

Figure 3. Box plots for recall results using NaCl as precursor salt for the classifiers proposed to predict pitting corrosion status of 316 L austenitic stainless steel

© 2015 WILEY-VCH Verlag GmbH & Co. KGaA, Weinheim

This graphical method is a useful tool to compare the influence of the .632bootstrap estimator, proposed by *Efron* and *Tibshirani* (1997), on the classification performance. When the models are trained with bootstrap technique, the training samples are obtained by replacement. In this way, as the Fig. 3 shows, when bootstrap was used, the values of recall were underestimated since about two thirds of the original data are used for training. Applying .632boostrap, the estimation got downward biased reducing the variability in the results. This can be demonstrated in the figure where the box size relative to the whiskers was thinner using .632bootstrap than using bootstrap for all the proposed models in this study. For this reason the .632bootstrap estimator was considered in this paper to compare the classification performance of the proposed models.

Table 2 depicts the mean estimation and standard deviation of recall and precision results for all the classification models. These values were obtained taking the average of all repetitions (40 times) for each model. Based on this table, the deviations from the mean values obtained for ANN were lower than those obtained for KNN. For ANN models, as the number of hidden neurons increased, the deviations were larger due to overfitting. In addition, the most accurate models were provided by ANN models when Bayesian regularization was considered since the deviation values for these models were the lowest. According to the collected results, the maximum value of recall and precision reached by KNN (recall = 0.956 and precision = 0.961) were obtained by the minimum value of k. For the data analyzed in this work, as the value of k increased, the performance of the KNN classifier decreased. On the other hand, the ANN models provided the maximum value in recall and precision terms when Bayesian regularization was considered (recall = 0.989 and precision = 0.996). According to the table, it can be observed that for the ANN models trained with *Levenberg-Marquadt* when the number of hidden neurons was larger than 2, the values of precision and recall decreased. In this case, too many neurons in the hidden layers may result in overfitting: the model presents so much information processing capacity that the limited information contained in the training set is not enough to train all the units taking part into the neural network. For the analyzed data, when Bayesian regularization was considered, ANN-BR, the overfitting was avoided since this technique causes the network to have smaller weights and biases, forcing the model response to be smaller and less likely to overfit. On the other hand, regardless the number of hidden neurons used in the structure, all the ANN models provided larger values of precision results than those obtained in recall term. This demonstrated the utility of these models to predict accurately the patterns that will suffer corrosion.

In order to compare the classification performance of the proposed models, the ROC space was used [16]. In a ROC plot, the true positive ratio (*TPR*, the proportion of original corrosion patterns that have been classified correctly) is plotted versus the false positive ratio (FPR, the proportion of original no corrosion patterns that have not been classified correctly). Therefore, the best models are those located closer to the upper left corner. Figure 4 shows the classification models represented in the ROC space.

According to the Fig. 4, the models based on ANNs outperformed KNN models. In addition, analyzing the upper left corner neighborhood, shown in the small area, it can be concluded that the ANN models trained with Bayesian regularization provided the best classification performance. Furthermore, Friedman test ($\alpha = 0.05$ level of significance) was applied to detect differences in the classification performance of these models. According to the value of the Friedman statistic ($p = 0.0916$ for TPR and $p = 0.6515$ for FPR), the null hypothesis was accepted (there were no significant differences between the ANN-BR models using different hidden neurons) and therefore, based on the principle of parsimony, the simplest configuration was selected as the optimal one. Therefore, in this case, the optimal structure for the ANN model was obtained with one hidden neuron using the Bayesian regularization.

Table 2. Mean and standard deviation values of recall and precision results. Optimal results for each classifier are in bold

Models	Recall	Precision
KNN		
k = 1	**0.956 ± 0.047**	**0.961 ± 0.041**
k = 3	0.940 ± 0.041	0.942 ± 0.044
k = 5	0.939 ± 0.041	0.927 ± 0.049
ANN		
4:1:2	0.984 ± 0.020	0.988 ± 0.045
4:2:2	**0.984 ± 0.022**	**0.993 ± 0.024**
4:5:2	0.977 ± 0.034	0.985 ± 0.034
4:10:2	0.964 ± 0.056	0.983 ± 0.035
4:20:2	0.919 ± 0.061	0.952 ± 0.050
ANN-BR		
4:1:2	0.987 ± 0.019	0.994 ± 0.022
4:2:2	0.987 ± 0.019	0.995 ± 0.019
4:5:2	**0.989 ± 0.018**	**0.996 ± 0.017**
4:10:2	0.989 ± 0.018	0.994 ± 0.022
4:20:2	0.989 ± 0.018	0.995 ± 0.020

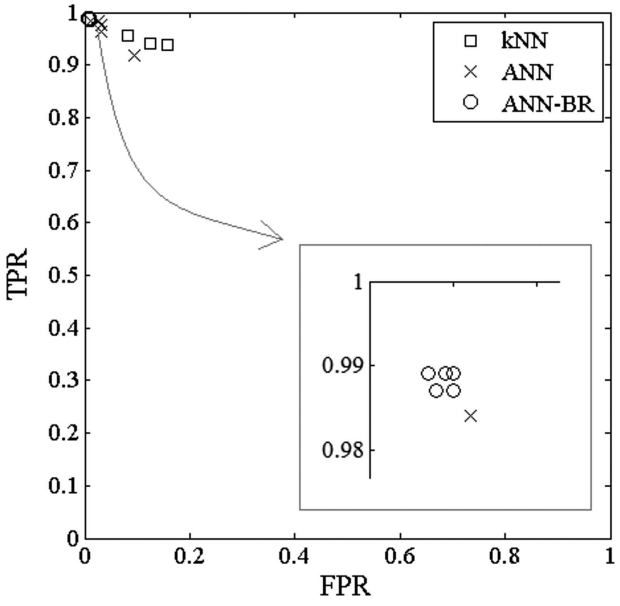

Figure 4. ROC space for all the classification models presented to predict pitting corrosion status of 316 L austenitic stainless steel

© 2015 WILEY-VCH Verlag GmbH & Co. KGaA, Weinheim

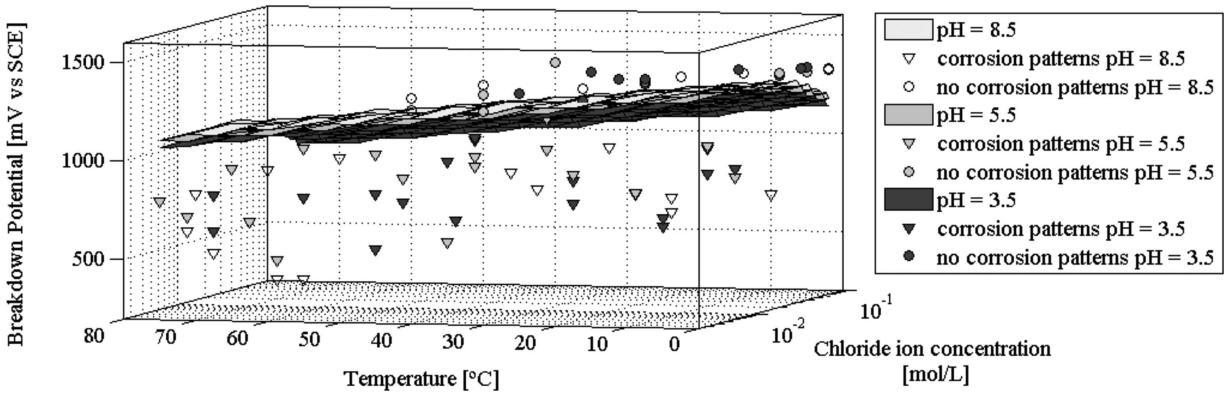

Figure 5. Pitting corrosion modelling using the best Bayesian ANN model for different pH values

Figure 5 shows the pitting corrosion modelling of 316 L austenitic stainless steel for different environmental conditions. The surface shown for each pH indicates the frontier between corrosion and no corrosion behavior. Each pattern, according to the environmental conditions, will have a corresponding breakdown potential. When this value of potential is below the surface, the material will suffer corrosion. On contrary, when the value of the potential is above the surface, the material will not suffer pitting corrosion. In this way, as it can be seen in the figure, the influence of the pH is not so relevant, however, the influence of the temperature is critical: when the temperature increases, the number of patterns suffering pitting corrosion is higher since the breakdown potential is lower and therefore, the patterns will have greater tendency to suffer pitting corrosion. This figure demonstrates the utility of the proposed model to predict pitting corrosion status of 316 L stainless steel in the range of environmental conditions considered in this work.

Comparing the presented results with those obtained in our previous work [20], the ANN-RB model outperforms the different models presented in that work, such as support vector machines (SVMs). In that case, the maximum value reached in term of percentage of cases correctly classified was 0.96. This comparison reflects the efficiency of the proposed model based on ANN-BR to predict pitting corrosion status of 316 L stainless steel. In addition, the performance of this model may be compared with those presented in *Jimenez-Come* et al. [21,22]. In those cases, the models (ANN and SVMs) were proposed to model pitting corrosion status considering only the environmental conditions (not considering the breakdown potential). The maximum value of precision reached by those models was 0.96, smaller than the maximum precision value obtained with ANN-RB in the presented study (precision = 0.996). This result reflects the importance of considering the breakdown potential values to model pitting corrosion status of 316 L stainless steel.

5 Conclusions

This paper presents a proposal for modelling pitting corrosion status of AISI 316 stainless steel using different classification models: KNN and ANNs. Polarization tests were undertaken to determine breakdown potential values studying different environmental parameters: chloride ion concentration, pH and temperature. These environmental conditions in addition to the breakdown potential values were used to construct the model with the ability to predict pitting attack on the material surface. Bootstrap was used to determine the optimal topology for the models. Based on recall and precision values, the most stable model was ANN-RB, performing with the highest classification success in most cases. This behavior was shown by the ROC space. The results demonstrated that Bayesian regularized neural network models are an excellent tool to obtain an automatic system to characterize pitting corrosion attack in stainless steel, resulting in the reliable prediction of corrosion status for this material without resorting to microscopic analysis.

Acknowledgements: This research has been performed with the support of Cátedra-ACERINOX (University of Cádiz) and the European Project "Avoiding catastrophic corrosion failure of stainless steel" (CORINOX RFSR-CT-2006-00022), developed partly in ACERINOX S.A., which kindly provided the authors with all the data and technical support. In addition, it is supported by a grant from European project FEDER-FSE 2007-2013. In addition, authors gratefully acknowledge the financial support provided by the project AC00178ETC from Knowledge Transfer Entity agent Andalusian Knowledge System. All contributions are greatly appreciated.

6 References

[1] K. H. Lo, C. H. Shek, J. K.L. Lai, *Materials Science and Engineering: R: Reports* **2009**, *65*, 39.
[2] L. Gardner, *Progress in Structural Engineering and Materials* **2005**, *7*, 45.
[3] D. Peckner, I. M. Bernstein, *Handbook of stainless steels*, McGraw-Hill, New York **1977**.
[4] M. H. Moayed, M. Golestanipour, *Materials and Corrosion*. **2005**, *56*, 39.
[5] A. J. Sedriks, *Corrosion of stainless steel*, WILEY, New York **1996**.
[6] R. Bhaskaran, N. Palaniswamy, N. Rengaswamy, M. Jayachandran, in: In *ASM Handbook Volume 13B*: *Corrosion: Materials*, ASM, Materials Park, OH, **2005**, p. 621.

© 2015 WILEY-VCH Verlag GmbH & Co. KGaA, Weinheim

[7] B. Deng, Y. Jiang, J. Gong, C. Zhong, J. Gao, J. Li, *Electrochim. Acta*. **2008**, *53*, 5220.
[8] E. Alfonsson, R. Qvarfort, *ACOM* **1992**, *3*, 1.
[9] R. Ovarfort, *Corros. Sci*. **1998**, *28*, 135.
[10] G. Salvago, L. Magagnin, M. Bestetti, *Electrochim. Acta*. **2002**, *47*, 1787.
[11] M. Ives, *Mater Charact*. **1992**, *28*, 257.
[12] M. Otieno, H. Beushausen, M. Alexander, *Materials and Corrosion* **2012**, *63*, 777.
[13] C. Andrade, J. Sanchez, J. Fullea, N. Rebolledo, F. Tavares, *Materials and Corrosion* **2012**, *63*, 1154.
[14] P. Wu, Z. Quan, J. Celis, *Materials and Corrosion* **2005**, *56*, 379.
[15] H. Mirzadeh, A. Najafizadeh, *Mater. Charact*. **2008**, *59*, 1650.
[16] R. A. Cottis, Q. Li, G. Owen, S. J. Gartland, I. A. Helliwell, M. Turega, *Mater. Des*. **1999**, *20*, 169.
[17] V. Díaz, C. López, *Corros. Sci*. **2007**, *49*, 949.
[18] D. Ok, Y. Pu, A. Incecik, *Ocean Eng*. **2007**, *34*, 2222.
[19] M. K. Cavanaugh, R. G. Buchheit, N. Birbilis, *Corros. Sci*. **2010**, *52*, 3070.
[20] T. Parthiban, R. Ravi, G. T. Parthiban, S. Srinivasan, K. R. Ramakrishnan, M. Raghavan, *Corros. Sci*. **2005**, *47*, 1625.
[21] S. A. Lajevardi, T. Shahrabi, V. Baigi, A. Shafiei, *Protection of Metals and Physical Chemistry of Surfaces*. **2009**, *45*, 610.
[22] M. Jiménez-Come, E. Muñoz, R. García, V. Matres, M. Martín, F. Trujillo, I. Turias, *Journal of Applied Logic* **2012**, *10*, 291.
[23] M. Jiménez-Come, I. Turias, J. Ruiz-Aguilar, F. Trujillo, *Materials and Corrosion* **2013**, *65*, 1024.
[24] M. Jiménez–Come, I. Turias, F. Trujillo, *Mater Des*. **2014**, *56*, 642.
[25] J. R. Galvele, in: R. P. Frankenthal and Jerome Kruger, (Eds.) *Passivity of Metals*, The Electrochemical Society, Inc., Princeton, N. J. **1979**, p 285.
[26] J. R. Galvele, *Treatise on Materials Science and Technology* **1983**, *23*, 1.
[27] S. Steels, *ASM Specialty Handbook*, ASM, Metals Park, OH **1994**.
[28] R. Merello, F. J. Botana, J. Botella, M. V. Matres, M. Marcos, Corros., *Sci*. **2003**, *45*, 909.
[29] N. J. Laycock, R. C. Newman, *Corros. Sci*. **1998**, *40*, 887.
[30] K. Hornik, M. Stinchcombe, H. White, *Neural Networks* **1989**, *2*, 359.
[31] C. M. Bishop, *Neural networks for pattern recognition*, Oxford University Press, Inc., New York, NY, USA **1995**.
[32] D. B. Fogel, *IEEE Transactions on*. **1991**, *2*, 490.
[33] K. Levenberg, *Q. Appl. Math*. **1944**, *2*, 164.
[34] D. E. Rumelhart, G. E. Hintont, R. J. Williams, *Nature* **1986**, *323*, 533.
[35] D. J. MacKay, *Neural Comput*. **1992**, *4*, 415.
[36] A. Tikhonov, *Soviet Math. Dokl*. **1963**, *5*, 1035.
[37] T. G. Dietterich, *Neural Comput*. **1998**, *10*, 1895.
[38] H. M. G. Smets, W. F. L. Bogaerts, *Mater Des*. **1992**, *13*, 149.
[39] B. Efron, R. Tibshirani, *Journal of the American Statistical Association* **1997**, *92*, 548.

(Received: December 3, 2014) W8173
(Accepted: January 2, 2015)

© 2015 WILEY-VCH Verlag GmbH & Co. KGaA, Weinheim